

Multiplexed label-free detection of single proteins

Contact philipp.kukura@chem.ox.ac.uk

A. Sebesta, A. Weigel and P.Kukura

Physical and Theoretical Chemistry Laboratory
University of Oxford
South Parks Road
Oxford OX1 3QZ

Introduction

Optical detection of single molecules usually relies on the fluorescent properties of the molecule or the introduction of a fluorescent label. Fluorescence detection of biological molecules such as proteins is often not possible without labelling due to their purely refractive nature in the visible and near infrared. Recently, alternative approaches eliminating the need of labels were introduced. These methods use the local refractive index sensitivity of surface plasmon resonances for sensing. Protein sensing down to the single molecule level was shown.^{1,2} These breakthroughs were achieved either by total internal reflection type dark field microscopy¹, or with photothermal microscopy using photoinduced heat dissipation to generate a refractive index contrast².

Limitations in dark field microscopy lie mainly in the efficient reduction of the background level. Multiple alternative approaches were developed to improve the background rejection of dark field microscopy, including the use of small rod mirrors^{3,4} or a perforated mirror⁵ in epi-illumination to introduce the excitation beam and reduce the background scattering. In addition, our group has shown recently, that a simple change in the illumination strategy can improve background rejection by two orders of magnitude compared to the state of the art, and enables imaging of single gold spheres down to 10 nm diameter in dark field.⁶

These methods exclusively relied on the readout of one gold nanoparticle sensor at a time. However, it would be desirable to extend these techniques to allow for multiple-particle read out and thus simultaneous observation of multiple events for implementing next-generation clinical diagnostic assays. Such essays would benefit from multiplexing possibilities and the ultimate single molecule detection limit. Schemes based on plasmon resonance shift detection of multiple particles were presented only recently. These techniques use either time gated events like a spatial light modulator in the conjugate image plane as a form of complex slit⁷, sample scanning⁸, or pure intensity readout⁹ to reach their multiplexing capabilities.

Here, we present a novel wide-field detection scheme, which allows us to simultaneously monitor the surface plasmon resonance of multiple gold nanorods. It directly records 2-dimensional, spectrally dispersed images of gold nanorod samples. The spectra are corrected via an overlapped particle image that correlates the particle positions to the reference slit position, allowing us to use the full 2D space of the sensor. We present an unprecedented low noise floor allowing us to observe single protein particle binding events with high signal to noise ratios.

Sample Preparation

Fibronectin from bovine plasma (F1141-1mg), and (3-Mercaptopropyl)trimethoxysilane (MPTMS) were bought from Sigma. Gold nanorods (25-47 nm) were bought from Nanopartz. Water (Elix®, Milipore) was filtered with 0.2 µm pore size filters before use. Microscope slides were bath-sonicated in a 1:1 isopropanol/water mixture and subsequently plasma-treated. The Microscope slides were then functionalized

with 2 v/v% MPTMS in acetone. Aqueous solutions of gold nanorods were spin-coated onto the functionalized microscope slides. The flow cell consists of a window 5 mm thick and 1 inch in diameter (UVFS AR= 350-700 nm, Thorlabs) with 2 holes connected to peek tubing (OD 1/16, ID 200 µm). A spacer made from silicon isolator sheet 0.8 mm in thickness and 1 inch in diameter (Grace Bio-Labs) with a flow channel 1 mm in width and 15 mm in length connects the window to the microscope slide. The entire flow cell is clamped to the microscope sample holder to ensure stability. Solutions are injected into the cell with a syringe.

Optical Setup

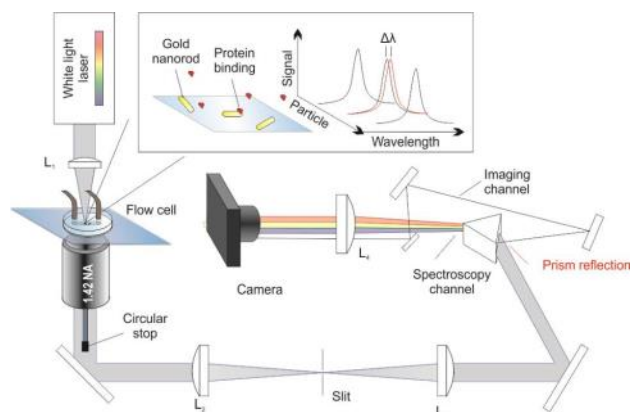


Figure 1 Experimental setup of the dark field microspectroscope. L1–L4: Achromatic lenses with focal lengths of $f_1 = 50$, f_2 and $f_3 = 150$ mm, and $f_4 = 500$ mm. Slit : can be closed to select spatial region and for calibration. Prism: Brewster-angle fused silica prism, to disperse scattered light and use the microscope in spectroscopy mode. The spectrum and image of the nanorods are imaged on the same camera. The inset shows a magnified region of the flow cell with 3 gold nanorods in a protein solution, and corresponding plasmon resonance spectra showing a plasmon resonance shift for the central nanorod.

The sample was illuminated by a commercial super continuum source (SuperK Extreme, NKT Photonics) with 40 MHz repetition rate. The microscope setup shown in Figure 1 is described in detail elsewhere⁶. Briefly, an achromatic lens ($f = 50$ mm) focuses the excitation beam under normal incidence onto the sample. At a spot size of 7–10 µm (full width at half-maximum), the power density was between 0.5 and 12 kW/cm². An oil-immersion objective with a numerical aperture of 1.42 (Olympus PLAPON 60x) collects scattered light together with the transmitted excitation light. The excitation beam is blocked after the objective by a 4 mm wide circular stop made of blackened aluminum. After the circular stop, a telescope consisting of two achromatic lenses L1 and L2 ($f = 150$ mm) enables spectral investigations with a slit in the focal plane. The beam then passes through a F2 prism (Thorlabs). The transmitted beam is dispersed and focused by a third achromatic lens ($f = 500$ mm) onto an EMCCD camera (QImaging Rolera Thunder), which records wide field spectral images of the sample. The reflected beam is picked off and sent slightly off axis through the same lens to create an overlapping spatial image. The image is shifted perpendicular to the spectral

dimension so that the particle image and the spectrum do not overlap on the camera. The dispersed mode provides two-dimensional images with a spatial axis in the vertical direction and a spectrally resolved axis in the horizontal direction. The effective pixel size is 96 nm/pixel for the spatial dimension and the spectral range was chosen from 555 – 675 nm to cover the surface plasmon resonance peak of the gold nanorods, with a spectral resolution of 0.17 to 0.3 nm/pixel in the blue and red region, respectively.

The system is calibrated by measuring a spectrum of a particle in the slit center, relating the spectral axis to the particle position. After this initial calibration the slit can be opened to allow for the observation of a larger region. For particles that are horizontally displaced from the slit center the corrected spectral axis can be obtained by shifting the current particle position to the known slit center position. This increases the available sensor space to the full region of the CCD.

Results

As explained in the previous section, there are no restrictions on the particle position in the field of view, i.e. the entire sensor can be used for spectrally resolved measurements. Spectra of particles away from the reference slit position can be corrected by referencing. The number of the observable particles in the field of view can be tuned by choosing the magnification, the chip size of the camera, and the dispersive element. The only restriction for unobstructed multiplexed imaging for particles at the same vertical (y) position that remains, is that the particles have to be sufficiently separated in the x dimension so that their spectra (2-3 FWHM) do not overlap. Particle spectra are obtained by binning of the vertical pixels. In aqueous solution, the spectrum is narrow with an approximately Lorentzian shape. Nonetheless, the spectrum is not symmetric. Hence, the particle spectrum is fitted with an antisymmetric, skewed Lorentzian, that is generated by composing the line shape out of two Lorentzians with two different widths, joint at the maximum. Our typical measurement noise of the plasmon maximum is 0.034 nm Δ LSPR, lower than reported in previous plasmonic single protein sensors.^{1,2,9}

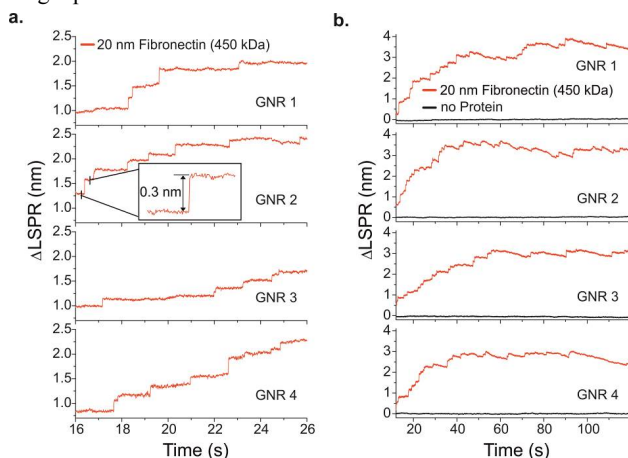


Figure 2 Time-dependent surface plasmon resonance shift for protein free (black) and 20 nM Fibronectin solution (red). A magnified region shows clear single protein binding steps, the inset emphasizes the unprecedented single to noise ratio (a). The full trace shows the saturation behavior after 1 min (b).

The sensitivity of our system with regards to single step protein binding is shown in Figure 2 by measuring Fibronectin, a 450 kDa protein. In this case the multiplexing is accomplished by measuring four nanorods simultaneously. A 22.8 nM solution of Fibronectin is injected into the system and the Δ LSPR is tracked simultaneous for all particles. Traces of protein-free solution (black) and protein solution (red) are shown for all particles and indicate the clear difference between signal to

background. There are no discernable step-like features for the control experiment. In contrast, the LSPR starts to shift for the protein solution immediately after injection of the analyte. A closer look at the early stage of the binding trace reveals that the LSPR changes in discrete steps. Furthermore, it can be seen that the steps are not correlated between different particles emphasizing the single protein nature of the measurements and the effect of the nanoenvironment. Only bound proteins influence the LSPR of the gold nanorods. In our case the nanorods are bare, and thus the proteins bind in a non-specific fashion to the unobstructed gold surface (approximately half of the rod). Individual steps show a broad distribution in magnitude, corresponding to the different binding sites on to the nanorods. This behavior can be explained by the difference electric field strength around the nanorod, being strongest at the tip of the rod and weakest at the sides. Hence, the strongest jumps can therefore be expected when the protein binds to the tip of the rod.¹⁰ In such cases we achieve a signal to noise ratio of >10 as shown in the inset. The overall response after saturation of all binding sites of the nanorods shows a similar overall shift in LSPR of 3.48 ± 0.41 nm for all nanorods.

Conclusions

We reported a simple method to measure the localized plasmon resonance shift down to the single protein level. Our method is capable of observing multiple particles simultaneously and thus enables the differentiation between correlated events over the full sample area and single molecule particle specific binding events. For Fibronectin (450 kDa) proteins we achieve a SNR of up to 10 depending on the binding site.

Acknowledgements

We thank the Central Laser Facility in Harwell for providing the SuperK Extreme continuum laser.

References

1. Ament, I., Prasad, J., Henkel, A., Schmachtel, S. & Sönnichsen, C. Single unlabeled protein detection on individual plasmonic nanoparticles. *Nano Lett.* **12**, 1092–5 (2012).
2. Zijlstra, P., Paulo, P. M. R. & Orrit, M. Optical detection of single non-absorbing molecules using the surface plasmon resonance of a gold nanorod. *Nat. Nanotechnol.* **7**, 379–382 (2012).
3. Sowa, Y., Steel, B. C. & Berry, R. M. A simple backscattering microscope for fast tracking of biological molecules. *Rev. Sci. Instrum.* **81**, 113704 (2010).
4. Nan, X., Sims, P. & Xie, X. S. Organelle tracking in a living cell with microsecond time resolution and nanometer spatial precision. *ChemPhysChem* **9**, 707–12 (2008).
5. Ueno, H. *et al.* Simple dark-field microscopy with nanometer spatial precision and microsecond temporal resolution. *Biophys. J.* **98**, 2014–23 (2010).
6. Weigel, A., Sebesta, A. & Kukura, P. Dark Field Microspectroscopy with Single Molecule Fluorescence Sensitivity. *ACS Photonics* **1**, 848–856 (2014).
7. Becker, J., Schubert, O. & Sönnichsen, C. Gold nanoparticle growth monitored in situ using a novel fast optical single-particle spectroscopy method. *Nano Lett.* **7**, 1664–1669 (2007).
8. Rosman, C. *et al.* Multiplexed plasmon sensor for rapid label-free analyte detection. *Nano Lett.* **13**, 3243–7 (2013).
9. Beuwer, M. A., Prins, M. W. J. & Zijlstra, P. Stochastic Protein Interactions Monitored by Hundreds of Single-Molecule Plasmonic Biosensors. *Nano Lett.* **15**, 3507–3511 (2015).
10. Shen, H. *et al.* Shape effect on a single-nanoparticle-based plasmonic nanosensor. *Nanotechnology* **24**, 285502 (2013).

